Published in final edited form as:
Proteins. 2012 August ; 80(8): 1948–1961. doi:10.1002/prot.24077.

Homology Modeling and Molecular Dynamics Simulations of the Active State of the Nociceptin Receptor (NOP) Reveals New Insights Into Agonist Binding And Activation

Pankaj R. Daga and **Nurulain T. Zaveri**
Astraea Therapeutics, LLC. 320 Logue Avenue, Mountain View, CA 94043

Abstract

The opioid receptor-like receptor ORL1, also known as the nociceptin receptor (NOP), is a Class A GPCR in the opioid receptor family. Although NOP shares a significant homology with the other opioid receptors, it does not bind known opioid ligands and has been shown to have a distinct mechanism of activation compared to the closely-related opioid receptors mu, delta and kappa. Previously reported homology models of the NOP receptor, based on the inactive-state GPCR crystal structures, give limited information on the activation and selectivity features of this fourth member of the opioid receptor family. We report here the first active-state homology model of the NOP receptor based on the opsin GPCR crystal structure. An inactive-state homology model of NOP was also built using a multiple template approach. Molecular dynamics simulation of the active-state NOP model and comparison to the inactive-state model suggests that NOP activation involves movements of TM3 and TM6 and several activation microswitches consistent with GPCR activation. Docking of the selective non-peptidic NOP agonist ligand Ro 64-6198 into the active-state model reveals active-site residues in NOP that play a role in the high selectivity of this ligand for NOP over the other opioid receptors. Docking the shortest active fragment of endogenous agonist nociceptin/orphaninFQ (residues 1–13) shows that the NOP EL2 loop interacts with the positively charged residues (8–13) of N/OFQ. Both agonists show extensive polar interactions with residues at the extracellular end of the transmembrane domain and EL2 loop, suggesting agonist-induced re-organization of polar networks, during receptor activation.

Keywords

GPCR; active conformations; molecular dynamics; MD simulations; orphanin FQ receptor; opioid receptor-like receptor; ORL1; NOP; opioid; extracellular loop 2; message; address

INTRODUCTION

The NOP receptor, previously known as the opioid receptor-like receptor ORL1, is a Class A GPCR, like other members of the opioid receptor family, and shares about 60% sequence homology with the opioid receptors. Its natural, endogenous ligand is a heptadecapeptide (FGGFTGARKSARKLANQ), called nociceptin or Orphanin FQ (henceforth referred to as N/OFQ), which has close resemblance to the endogenous kappa opioid receptor agonist, dynorphin. Functional activation of NOP, like the entire class of opioid receptors, results in

ADDRESS CORRESPONDENCE TO: Dr. Nurulain T. Zaveri, Astraea Therapeutics, LLC., 320 Logue Avenue, Suite 142, Mountain View, CA 94043, Tel: 650-254-0786, Fax: 650-254-0787, nurulain@astraeatherapeutics.com.

SUPPORTING INFORMATION

NOP receptor amino acid numbering according to the Ballesteros-Weinstein convention and alignment of the NOP and opioid receptor sequences are contained in the Supporting Information.

inhibition of cAMP synthesis and stimulation of K^+ conductance. However, that is where the similarities end, because none of the endogenous or synthetic opiates that bind to the opioid receptors have high affinity for the NOP receptor,[1] and the reverse is also true. Clearly, the functional architecture and activation mechanism of the NOP receptor differs from those of the other opioid receptors. Understanding these differences is crucial for a comprehensive rational drug design approach for selective NOP ligands, which in turn are important for a complete understanding of the NOP system as a drug target in pathophysiological states. Site-directed mutagenesis studies have aided significantly in understanding the differences in binding site architecture among opioid receptors and NOP; however, nothing is yet known about the activation process after receptor binding, particularly with respect to small-molecule binding and activation.

The first homology model of the NOP receptor was published by Topham et al. using the bovine rhodopsin model of Herzyk and Hubbard as a template for the seven transmembrane (TM) helices.[2] Modeling the complex between the NOP receptor and its peptide ligand N/OFQ showed that the N-terminus binds to a conserved region in the transmembrane binding pocket, whereas the positively charged core, N/OFQ (8–13) makes selective interactions with the NOP extracellular loop 2 (EL2).

Non-peptidic small-molecule NOP receptor ligands have also been docked into the NOP homology model constructed based on the Palczewki bovine rhodopsin crystal structure[3] and more recently, on the beta2-adrenergic receptor.[4] In both instances, NOP agonist ligands (Ro 64-6198 in the former, and a spiropiperidine-based NOP agonist in the latter) were docked into the homology model of the inactive form of the NOP GPCR. These NOP agonists also bind in the TM binding pocket and appear to make interactions with the same receptor residues as the N-terminus residues of the N/OFQ peptide; however, these small-molecule agonists do not appear to interact extensively with the EL2 loop in these models.

Unlike the other opioid receptors, the EL2 loop of NOP is extremely crucial for binding selectivity and particularly the activation of the NOP receptor.[5,6] However, the NOP homology models published thus far do not directly indicate whether the EL2 loop is involved in activation by small-molecule ligands especially full agonists such as Ro 64-6198.

Given the recent availability of the crystal structure of an activated GPCR, the opsin receptor, we report here, the first homology model of the active-state of the NOP receptor, built using the opsin receptor as a template. We also report an inactive-state homology model of the NOP receptor, based on the beta2 adrenergic receptor and rhodopsin as templates. A comparison of the active and inactive models of the receptor suggests that the NOP receptor activation follows a similar activation switch pathway as proposed for other GPCRs.[7–10] A unique feature of the NOP receptor is its anionic EL2 loop, which we show plays a role in binding the cationic core (8–13) of the N/OFQ heptadecapeptide and is key to the activation process of NOP, unlike other receptors in the opioid receptor family. We docked the agonist heptadecapeptide N/OFQ and the small-molecule agonist Ro 64-6198 into the active receptor. Both these agonists are engaged in polar interactions with residues at the extracellular end of the transmembrane domain, consistent with agonist-induced re-organization of polar networks during receptor activation, lending further insights into the role of the EL2 loop interactions in the activation process.

METHODS (COMPUTATIONAL DETAILS)

Homology modeling of NOP receptor

Amino Acid Numbering System—GPCR residues are labeled using the Ballesteros Weinstein numbering, except for loop regions where crystal structure numbering is used. Residues in the TM domain are assigned two numbers (n1.n2), wherein "n1" represents TM helix number, while "n2" represents the number relative to the most conserved residue in the TM, which is assigned 50 (numbers decreasing towards N-terminus and increasing towards C-terminus). The conserved residues in the NOP receptor TM domains are N69 (TM1), D97 (TM2), R148 (TM3), W175 (TM4), P227 (TM5), P278 (TM6) and P316 (TM7) (See SI Figure S1 for NOP numbering). In some cases, the well-known NOP receptor amino acid residues are labeled with the residue number of the amino acid with a superscript of the Ballesteros Weinstein number as exemplified by $Asp130^{3.32.}$ Amino acid residues of the heptadecapeptide agonist ligand, N/OFQ, are labeled with the single alphabet abbreviations.

Homology modeling—The homology models of the NOP receptors were built with the 'Advanced Protein Modeling' (APM) module in SybylX1.1 (Tripos Inc). The APM module of SybylX1.1 is based on ORCHESTRAR, which is comprised of a suite of applications for knowledge-based comparative modeling.[11–13] The model of the inactive conformation of the NOP receptor was constructed using the crystal structures of antagonist-bound β2 adrenergic receptor (AR) (PDB code: 2RH1.pdb)[14] and the rhodopsin structure (PDB code: 1F88.pdb)[15] as templates.[16]

A comparative model of the active-state conformation of NOP was built using crystal structure of G-protein bound opsin (Ops*) as a template (PDB Code: 3CAP.pdb).[17] The Ops* structure represents the activated form of this GPCR.

Model building—Sequence alignment was carried out with ClustalW. The alignment obtained was edited manually to remove insertions within the alpha helices and to align the highly conserved motifs such as the DRY motif in the transmembrane helix 3 (TM3) and NPxxY motif in TM7. The manually edited sequence alignment of the NOP sequence with the sequence of opsin receptor is shown in Figure S2 in the Supporting Information. The sequence alignment of NOP with the mu, delta and kappa opioid receptor GPCRs is provided in the Supporting Information as Figure S3.

EL2 loop building—Modeling the EL2 loop is an important part of the NOP model construction, since the EL2 loop in the NOP receptor has been shown to be very important for binding the endogenous ligand and activation of the receptor.[5,6] The secondary structure of the EL2 loop in β1 and β2 AR is α-helical, whereas it is a β-strand in bovine rhodopsin. Secondary structure prediction methods suggest a β-strand hairpin-like structure for the EL2 loop in NOP.[18–20] The rhodopsin template was therefore used to build the EL2 loop in NOP.

The EL2 loop was constructed in a step-wise manner. First a peptide chain was constructed by manual extension of the TM4 extracellular end till residue Glu202 (two residues after conserved Cys200) and N-terminal of TM3. Once the position of Cys200 was tentatively fixed, a loop search was carried out using the Biopolymer module in SybylX1.1, for loops between Cys200 and N-terminal of TM3 as well as between Cys200 and C-terminal of TM4. Twenty-five loops were generated for each fragment. From these, the best loops were selected based on the homology with the template as well as the conformation of loop. Energy minimization was carried out after each step to remove bad geometries and steric clashes with other amino acids in the receptor model.

Final Model Refinement—The "Biopolymer Structure Preparation" protocol in SybylX1.2 was used to add hydrogen atoms to the models. The N- and C-terminals were capped with a charged NH_4^+ and COO^- groups respectively. Finally, the models were subjected to stepwise minimization, which included hydrogen minimization, side-chain minimization, and backbone minimization, followed by complete model minimization. All the energy minimizations were carried out using AMBER7 FF02 force field available in SybylX1.2 with Amber charges. The distance-dependent dielectric constant of 4 was used for the minimization. All models were validated and analyzed using PROCHECK and proSA-web server.

Molecular Dynamics (MD) Simulations

Unliganded active and inactive receptor—The NOP receptor homology models were subjected to MD simulations using NAMD[21] to test the overall stability of the models. The MD simulations were performed using the parameter set 22 in CHARMM.[22] The receptors were embedded in a 1-palmitoyl-2-oleoyl-phosphatidylcholine (POPC) membrane bilayer which consisted of solvated POPC molecules. The initial equilibrated bilayer contained 8 × 8 × 2 POPC molecules. The receptor models were placed in the center of the lipid bilayer such that the extracellular and intracellular loops were at the lipid water interface. A total of 8,347 water molecules (8348 for inactive state conformation) were used to solvate the entire system. Lipid molecules overlapping with the receptor were then removed. The system was then solvated with water, and random water molecules were replaced by potassium or chloride ions to achieve electroneutrality and a physiological ionic strength of 0.15M. The entire assembly contained 45,710 atoms (45,909 for inactive state conformation). The entire assembly was then subjected to energy minimization for 5000 steps to remove close contacts between receptor atoms and the solvent or lipid layers.

The entire system was heated in stepwise manner from 0K to 310K in the increments of 25K for each 10 ps. The system was then subjected to the first simulation, equilibration phase (500 ps). The protein backbone atoms were maintained in fixed positions throughout the heating and equilibration steps, to allow water molecules to enter the receptor. During this process, lipids in contact with the protein can orientate correctly. In the next step of equilibration, all atoms, except the Cα atoms of the receptor, were relaxed and the system subjected to a Cα-constrained MD simulation for 1 ns. For the production stage, all atoms in the assembly were relaxed and the whole system subjected to MD simulation for a total of 8 ns. Periodic boundary conditions were applied, and the Nosé-Hoover Langevin piston pressure control for temperature and pressure coupling was adopted. The production run was was performed at constant temperature (310 K) and pressure (1 atm.) using a 1 fs time-step for integration. The Particle Mesh Ewald method (PME) was used to calculate the electrostatic contribution to non-bonded interactions with a cutoff of 12 Å and a time step of 1 fs. The cutoff distance of the van der Waals interaction was 12.0 Å. The SHAKE algorithm was applied to the system. Visualization and graphical analysis of the trajectories were performed with the VMD software.[23] Distance measurements, RMSD calculations and further trajectory analyses were carried out using ptraj module in AmberTools1.5.

Modeling of N/OFQ:Nociceptin Complex

Orsini et al. investigated the NMR solution structure of nociceptin in a membrane-like environment and suggested that the N/OFQ peptide exists preferably in a stable helix conformation from residues 5–17 whereas the functionally important N-terminal residues (message domain) folded aperiodically on top of the helix.[24] A three-dimensional structure of the N/OFQ peptide was built using the Biopolymer module in SybylX1.2. The first five amino acids were built as a random coil (with an extended conformation) while the remaining peptide was built to have an α-helical structure.

After MD simulation of the active conformation of the NOP receptor, the EL2 loop acquired a β-sheet conformation, and is positioned, like a lid, on top of the binding cavity comprised of TM3, TM5, TM6 and TM7 residues. For N/OFQ to bind to the NOP receptor, a movement of the hairpin-like structure of the EL2 loop is necessary. The N/OFQ peptide was manually docked into the stable activated NOP model obtained after MD simulation. The positively charged nitrogen of F1 was positioned in close proximity of Asp130$^{3.32}$. The complex was then minimized using the MMFF94 force field and charges and distance-dependent dielectric constant of 1. The entire complex was then subjected to molecular dynamics simulations using NAMD with a similar protocol as described above for the inactive and active apo receptor structures. The production run was carried out for 4 ns.

RESULTS AND DISCUSSION

Validation of the NOP homology models

The NOP models showed the characteristic topology of the 7TM helices common to most class A GPCRs. The root mean square deviation (RMSD) of the initial active-state model with the template structure (the opsin crystal structure 3CAP.pdb) was found to be 2.27 Å. Higher deviation of the model structure was observed within the loop region. The comparison of the transmembrane helices revealed that the RMSD in the transmembrane helices was less than 0.5 Å. The RMSD of the final refined structure (after minimization) from the initial model was 1.065 Å (1.26 Å for inactive). The final refined models were validated using PROCHECK analysis. The Ramachandran plots of the models suggested that 85.5% of the residues resided in the most favored regions in the active conformation (83.3% for NOP in inactive conformation), 13.7% (13.7% for NOP in inactive conformation) in additionally allowed regions, and 0.8% (only two residues) (1.1% for NOP in inactive conformation) in the generously allowed regions. No residue was found in the disallowed regions in the active conformation, while about 5 residues (1.9%) were found in disallowed region in the inactive conformation. We also validated the models using the ProSA-web server (https://prosa.services.came.sbg.ac.at.). The ProSA-web z-scores of the models were compared to those of the templates and were found to be within the acceptable range.

Inactive Conformation of the NOP receptor

The inactive-state NOP receptor model was built using Advanced Protein Modeling in SybylX1.2. The receptor model showed most features common to the inactive conformation of GPCRs, as reported for the antagonist- and inverse agonist-bound crystal structures of various GPCRs.[14,25–28] The active site, located near the conserved residue Asp130$^{3.32}$ is made up of residues from TM3, TM5, TM6 and TM7, and the EL2 loop is positioned as a lid on top of the binding pocket. The unliganded, inactive-state NOP receptor model also showed most GPCR activation micro-switches in their ‘inactive positions’ and distinct from that in the active-state model (*vide infra*). The indole side-chain of Trp276$^{6.48}$ was present in its inactive conformation, positioned ‘vertically down’ at the bottom of main ligand-binding site. This Trp276$^{6.48}$ belongs to the conserved CWxP motif, located in the middle of TM6. The Trp6.48 of the CWxP motif (Trp276 in NOP) is believed to function as an activation micro-switch, and is involved in the movement of TM6 upon agonist binding.[9,10]

Asp147$^{3.49}$ and Arg148$^{3.50}$ of highly conserved DRY motif located at the cytoplasmic end of TM3, were found to be involved in a salt bridge interaction. Arg148$^{3.50}$ functions as another activation micro-switch, which, in the active-state, agonist-bound receptor, forms an ionic interaction with a Tyr residue from TM5. The ionic interaction of Arg148$^{3.50}$ with Asp147$^{3.49}$ serves as an “ionic lock” for the inactive conformation of Arg148$^{3.50}$. This ionic interaction is not present in the active-state conformation of the NOP model or in the opsin

template, consistent with the activation-related ionic interaction with the Tyr from TM5 (*vide infra*).

The highly conserved residue Tyr319$^{7.53}$ of the conserved NPxxYmotif constitutes an important micro-switch in the activation of the class A GPCRs, by interchanging between two or three different side-chain rotamers.[10] All the GPCR crystal structures reveal an internal polar hydrogen bonding network on the inner side of the helical bundle. Our models showed a similar H-bonding network. Asn315$^{7.49}$ and Tyr319$^{7.53}$ of the NPxxY motif are involved in an extended hydrogen bond network between TM3 and TM7. This extended polar network also includes Asp97$^{2.50}$, Ser137$^{3.39}$ and Asn311$^{7.45}$. In the inactive conformation of the NOP receptor, one of the important amino acids involved in the hydrogen bond network, Asp97$^{2.50}$, showed a hydrogen bond interaction with Asn133$^{3.35}$. This interaction was observed only in the inactive NOP model but not in active-state model. Mutagenesis of Asn133$^{3.35}$ to a Trp residue resulted in a constitutively active mutant, without affecting the binding affinity of N/OFQ.[29] These results suggest that the disruption of the participation of Asn133$^{3.35}$ to the hydrogen bond network may contribute to the activation of the NOP receptor. The presence of a hydrogen bond interaction of Asn133$^{3.35}$ in our inactive model but not in the active-state model is consistent with the results of the mutagenesis studies carried out by Kam et al.[29]

Active-State Conformation of the NOP receptor

The active-state NOP receptor model shows all the features possessed by the active conformation of class A GPCRs.[30,31] A comparison between the inactive and active conformations (Figure 1) showed the classical TM movements associated with GPCR activation. The intracellular end of the TM4 in active conformation moved towards the helical bundle, while the extracellular end remained unchanged. Compared with the inactive structure, the TM6 in the active NOP receptor conformation is tilted away from helical bundle. This movement is necessary during activation of GPCR to accommodate the C-terminal end of the G-protein within the groove of the helical bundle at the intracellular end. The extracellular half of TM7 moved towards the binding site while the intracellular half moved away from the TM helical bundle (Figure 1C). Similar to the Ops* crystal structure, the TM5 is elongated by 2 helical turns, towards the intracellular end, in the active conformation.

The slight movement of the extracellular end of TM3 away from the binding site resulted in a simultaneous movement of the EL2 loop away from its actual position in the inactive conformation (Figure 1B), thus generating enough space between EL2 and EL3 loops to accommodate the N/OFQ peptide. This movement of the EL2 loop enables the negatively charged amino acid residues Glu194, Asp195, Glu196, and Glu197 to orient towards the opening of the ligand binding pocket, thus allowing the possible interations with the incoming positively charged N/OFQ peptide. Particularly, the side chains of the residues Glu194 and Asp195 were found to be facing the opening within EL2 and EL3 loop. These negatively charged EL2 loop residues have been shown to be crucial for activation of the NOP receptor but not the closely related KOP receptor.[5,6]

Activation micro-switches in the NOP receptor active-state model

The active-state NOP model, based on the opsin template, showed no ionic interaction between Asp147$^{3.49}$ and Arg148$^{3.50}$, the ‘ionic lock’ of the conserved DRY motif. In the active-state NOP model, Arg148$^{3.50}$ showed a H-bonding interaction with Tyr235$^{5.58}$, which is characteristic of the active conformation of GPCRs.[9] The Asp147$^{3.49}$ of DRY motif now showed a salt-bridge interaction with Lys166$^{4.41}$ from TM4. Asp147$^{3.49}$ was also involved in a hydrogen bonding network with Tyr89$^{2.42}$ from TM2. The polar hydrogen bonding

network, similar to that found in the inactive-state of NOP receptor, was retained in the active conformation of NOP receptor. However, the slight movement of TM3 in active conformation resulted in the movement of Asn133$^{3.35}$ away from the polar residues and the hydrogen bond between Asn133 and Asp97 was disrupted. The movement of TM3 and the disruption of the hydrogen bond interaction of Asn133 during the activation process is consistent with mutagenesis data that the N133W mutant of the NOP receptor is constitutively active.[29]

Interestingly, although the highly conserved residue Trp276$^{6.48}$, the well-known 'rotamer toggle switch for TM6' was translocated toward TM5 during the movement of TM6, its indole side-chain was still in its "vertically down" inactive-state conformation. This is similar to what is observed for Trp6.48 in the opsin template from which the NOP receptor active conformation was built. During molecular dynamics simulation of the NOP active model, there is a prominent rotation of the indole side-chain of this 'W6.48 toggle switch' to the 'active (up)' conformation, thereby allowing the movement of TM6 and the stabilization of the 'aromatic lock' between Phe224$^{5.47}$ and the Trp276$^{6.48}$ indole side chain. These molecular movements are possibly a part of the NOP activation process and are consistent with those observed with other GPCRs.

The comparison of active and inactive conformation of NOP receptor revealed that the Met134$^{3.36}$ might play an important role in NOP receptor activation. The bulky and hydrophobic side-chain of Met134$^{3.36}$ might be responsible for the holding the Trp276$^{6.48}$ in its inactive conformation. The two residues reside in very close contact with each other, thus restricting the movement of the Trp276$^{6.48}$ toggle switch, required for the activation of receptor. The size of this residue at position 3.36 in TM3 appears to play a role in the constitutive activity of GPCRs. The highly constitutively active receptors have smaller residues at 3.36 position; for example, Ser in ghrelin receptor. Other constitutively active receptors such as GPR39 (Ser), GPR119 (Ala), NK1 (Ala), β1- and β2-adrenergic (Val) and 5-HT4 (Thr) also have smaller residues at this corresponding position. Site-directed mutagenesis studies of the 5HT4 receptor have shown that basal constitutive activity results from stabilization of the double toggle switch of Thr3.36 and Trp6.48.[32] A similar observation was also reported with the CB1 receptor, wherein Phe201Ala$^{3.36}$ mutant shows greater constitutive activity than the wt receptor, suggesting importance of the size of the 3.36 residue in the ligand-independent activation of class A GPCRs.[33] The movement of Met134$^{3.36}$ during NOP receptor activation is further discussed below.

Molecular Dynamics Simulation

MD simulations on both the inactive-state model as well as the active-state model were carried out to fully understand the structural changes upon NOP activation. The RMSD of atoms from the initial structure serves as an important measure to check the stability and overall movement of the TM helices. The initial active-state model of the NOP receptor was used as the starting structure. The RMSD was calculated for each MD snapshot (one every 1 ps) after the coordinates of the final structure were superimposed on the coordinates of the starting structure. The energy-minimized structure obtained from the NAMD energy minimization step was used as the reference structure for calculation of the RMSD for each MD snapshot.

The overall RMSD of the active-state homology model after a 8 ns MD simulation was ~2.0 Å. As seen in Figure 2, the model rapidly deviated from the initial structure during the first two nanoseconds of the simulation run. This increase in the RMSD was due to optimization of interactions within the protein structure, as well as with the lipid bilayer and solvent molecules. After ~2.0 ns, the total RMSD stabilized at 2.0 Å and represented a satisfactory

and stable structural model. The MD simulation of the inactive-state model showed similar RMSD of ~2.5 Å (not shown).

The binding site architecture of the active as well as inactive conformations of the NOP receptor remained quite conserved throughout the trajectory. During the MD simulation of the inactive conformation, one of the side-chain O of the conserved Asp130$^{3.32}$ showed a hydrogen bond interaction with side-chain phenolic OH of Tyr309$^{7.43}$. We found that this interaction was preserved (>90% occupancy) throughout the simulation (Figure 3, upper panel). This interaction brings TM3 and TM7 in close proximity. However, this hydrogen bond interaction between the two amino acids was broken after about 3 ns during the MD simulation of the active conformation (Figure 3, lower panel). This observation during the MD simulation is consistent with the proposed "3–7 lock" observed between D$^{3.32}$ and Y$^{7.43}$ of the three opioid receptors mu, delta and kappa, during MD simulations reported by Kolinski and Filipek.[34,35] They reported that the hydrogen bond interaction between the Asp130$^{3.32}$ and Tyr309$^{7.43}$ from TM3 and TM7 is preserved during their MD simulation of antagonist:receptor complexes (inactive conformation) and broken during simulation of agonist:receptor complexes (active conformation). The breaking of this '3–7 lock' in the activated NOP receptor results in a slight movement of the TM7, opening a small pocket in the TM domain. This newly observed pocket is in close proximity of the Met134$^{3.36}$ in TM3, and is now occupied by hydrophobic side-chain of Met134$^{3.36}$ during MD simulation. The movement of Met134 thus provides enough space to swing the indole side-chain of Trp27$^{6.48}$ during the seesaw movement of TM6 (rotamer toggle switch) (*vide infra*).

A significant 'activation-related' movement was further observed during the MD simulations of the active-state conformation. The indole side-chain of the Trp276$^{6.48}$ of the conserved CWxP motif of TM6, which in the active-state model prior to MD simulation, still appeared to be in its 'inactive' rotamer (*vide supra*), now moves to a position towards TM5, in line with the 'rotamer toggle switch' mechanism for TM6 movement during GPCR activation. Further, the Trp276$^{6.48}$ showed a π-stacking interaction with Phe224$^{5.47}$ of TM5. Recent studies by Holst et al have demonstrated that the rotation around the chi1 torsion angle of Trp6.48 (during activation) brings its side-chain close to the highly conserved Phe5.47 in TM5, which serves as an "aromatic lock".[36] The active-state NOP receptor model after MD simulation showed this characteristic aromatic lock, which presumably locks the Trp276$^{6.48}$ rotameric switch in an active conformation, triggering the global movement of TM5 and TM6 during the receptor activation process.

Significance of Second Extracellular Loop (EL2) of the NOP Receptor

The NOP receptor and the kappa opioid receptor (KOP) and their cognate ligands share greater structural similarities with each other than with the other members of the opioid receptor family (mu and delta opioid receptors MOP and DOP respectively). However, studies with NOP-KOP chimeric receptors show that the NOP receptor uses an activation mechanism markedly distinct from the KOP receptor, and that the EL2 loop is an absolute requirement for activation of the NOP receptor but not the KOP receptor.[5,6] The importance of the NOP EL2 loop residues have not yet been studied with site-directed mutagenesis, however, the active-state model and MD simulations presented here lend some insight into the role of the EL2 loop of the NOP receptor in binding of the N/OFQ ligand, receptor activation and possibly selectivity of NOP ligands over the other opioid receptors.

The involvement of the EL2 loop in receptor activation has been shown for several GPCRs. The residues of EL2 loop in the M3 muscarinic acetylcholine receptor[37] and V(1a) vasopressin receptor are reported to be essential in receptor function and activation.[38] In the GnRH receptor, mutation of two residues in the EL2 loop converted an antagonist to an agonist, indicating their significance in receptor activation.[39] With the 5-HT4 GPCR,

circular dichroism and steady-state fluorescence studies showed that receptor activation was distinctly coupled to a change in the conformation of its EL2 loop.[40]

After MD simulation of the active-state NOP receptor, the EL2 loop acquired a β-sheet conformation (shown as orange colored hairpin like structure, in Figure 5B), and is positioned as a lid on top of the binding cavity over TM3, TM5, TM6 and TM7.

The Cys200 in the middle of the EL2 loop forms a disulfide bridge with the Cys123$^{3.25}$ on the extracellular end of TM3. The movement of TM3 during activation is therefore accompanied by the movement of EL2 loop. The movement of EL2 loop results in a forward movement of Glu197 and Glu199, bringing them in closer proximity to TM7. Here they make strong ionic interactions with Arg302$^{7.36}$ from TM7, and H-bonding interactions with Tyr309$^{7.43}$ from TM7 and Tyr58$^{1.39}$ of TM1 (Figure 6A). The position and side-chain of Glu199 is restricted to a certain extent because of the neighboring amino acid, Cys200, which is constrained by the disulfide bond with Cys123$^{3.25}$. This hydrogen-bonding network between TM1 and TM7 and the negatively charged amino acids of the EL2 loop seems to stabilize the active-state of the NOP receptor. Both Tyr309$^{7.43}$ and Tyr58$^{1.39}$ are conserved throughout the opioid family. Mutation of Tyr$^{7.43}$ in the opioid receptors (MOP, KOP and DOP) resulted in a decrease in binding affinity of opioid agonists and antagonists.[41] Although mutation studies for the Tyr309$^{7.43}$ in NOP have not yet been reported, one can expect a similar trend for the NOP receptor, suggesting the importance of the Tyr309$^{7.43}$ in stabilizing the NOP binding site. The Arg302$^{7.36}$ residue, on the other hand, is unique to the NOP receptor. The corresponding amino acid in MOP and DOP is His (Tyr in KOP). The ionic interaction between Arg302$^{7.36}$ and Glu199 (EL2) might play a significant role in importance of the EL2 loop in the NOP activation process. This, in addition to the H-bonding interaction of Glu199 with Tyr309$^{7.43}$ and Tyr58$^{1.39}$, hold the EL2 loop over the helical assembly of the NOP receptor and may contribute to the importance of the EL2 loop in binding and possibly even selectivity of NOP ligands for the NOP receptor over the other opioid receptors.

A comparison of the amino acids at the extracellular end of the binding cavity and the EL loops of the four GPCRs in the opioid receptor family possibly explains the differences in the EL2 loop conformation between NOP and the other opioid receptors, and consequently its importance and participation in ligand binding and receptor activation. For instance, a relatively smaller amino acid residue Leu301$^{7.35}$ at the N-terminal of TM7 in NOP allows the EL2 loop to locate itself in close proximity of TM6 and TM7. The corresponding amino acid in MOP is Trp320, located at the extracellular end of TM7 of MOP. The steric bulk of Trp320 (Tyr312 in KOP) would likely create steric hindrance with the EL2 loop in these opioid receptors, thus preventing its close proximity to TM1 and TM7 or movement towards TM3 during activation. Even the Arg302$^{7.36}$ residue in NOP is more flexible than corresponding amino acid residues in MOP (His321) and KOP (Tyr313). These larger aromatic residues in MOP and KOP as well as lack of flexible basic residues result in a different EL2 loop conformation in KOP and MOP receptors. Therefore, the EL2 loops of KOP and MOP do not participate in activation or ligand binding to these receptors, in contrast to the EL2 loop in NOP (Figure 6B).

Complex of Active-state NOP receptor conformation with its cognate peptide ligand N/OFQ

Previous reports of the N/OFQ binding to the NOP receptor homology model used the inactive-state conformation of the NOP receptor, since these were carried out prior to the crystal structure reports of active-state GPCRs.[2,42] In our study, N/OFQ (1–17) was manually placed into the NOP active-state binding pocket, as described in the Methods and the receptor-ligand complex was subjected to a 4ns MD simulation. Since the EL2 loop in the NOP model sits on top of the TM binding pocket, a movement of the EL2 loop is

required, for the ligand to access the binding pocket. Two possible movements of EL2 can be assumed, one being the movement of the hairpin towards EL3 loop (shown as a green coil) thus opening the channel between the EL2 and EL1 (cyan in Figure 7A) loops. However presence of the disulfide bond between Cys123$^{3.25}$ and Cys200 restricts the movement of EL2 hairpin-like structure away from EL1 loop. Furthermore, since the residues forming the EL1 loop in the other opioid receptors are very similar and highly conserved, it is unlikely that the EL1 loop is involved in the binding of N/OFQ. The other possibility is the movement of EL2 loop towards the EL1 loop, thus opening the channel between the EL2 and EL3 loop. The movement of the EL2 loop to accommodate the N/OFQ peptide binding enables the negatively charged amino acid (E194-D195-E196-E197) residues to orient towards the binding cavity, thus allowing the possible interactions with positively charged residues (8–13) of the incoming N/OFQ peptide. The location of three extracellular loops and possible binding of nociceptin helical structure is shown in the Figure 7A below.

The binding mode of N/OFQ (1–13) (shown in Figure 7B) is mostly consistent with that proposed earlier by Topham et al with the inactive-state NOP model.[2] The N/OFQ residues 14–17 did not appear to make interactions with the receptor, even after MD simulation. This is consistent with the SAR studies showing that the shortest active fragment of N/OFQ is NC(1–13)NH2.[43,44] The N-terminal F^{1}G^{2}G^{3}F^4 message domain of N/OFQ appears to have an extended conformation and binds to the expected ‘opioid’ binding pocket. The ionic interaction between the positively charged terminal nitrogen of F1 of N/OFQ with the negatively charged Asp130$^{3.32}$ was maintained throughout the MD simulation, as shown in the graph in Figure 8. This interaction with Asp130$^{3.32}$ has been shown to be a necessary requirement for NOP receptor activation.[45] F1 of N/OFQ occupied the pocket between Phe224$^{5.47}$ and Trp276$^{6.48}$. Site-directed mutagenesis of Phe224$^{5.47}$ to Ala224 yielded a mutant receptor which had significantly reduced affinity for N/OFQ and ~200 fold reduced potency for activation. Mutation of Tyr131$^{3.33}$, Phe220$^{5.43}$, and Trp276$^{6.48}$ also reduced the binding affinity and potency of N/OFQ, but to a lesser extent in comparison to F224A mutation.[45] Although Phe220$^{5.43}$ lies near the F1 binding pocket, it showed very limited contact with the F1 residue of N/OFQ. Consistent with mutagenesis data, two polar residues Ser223$^{5.46}$ and Gln280$^{6.52}$ located near F1 pocket also make very limited contact with N/OFQ, and their mutation does not affect N/OFQ binding or potency.[42,46] However, Gln280$^{6.52}$ mutation to His (corresponding residue in opioid receptors) increased the affinity of opioids lofentanil and etorphine for the NOP receptor, indicating the importance of this His residue to opioid recognition and suggesting why the NOP receptor does not recognize opioid ligands.[46]

T5-G6-A7 of the N/OFQ peptide binds to the interface between the transmembrane helices and the EL2 loop. Consistent with interactions observed in the Topham model, the polar sidechain of T5 was involved in hydrogen bonding interaction with Gln286, located at the extracellular end of TM6. During MD simulation, the sidechain -OH of T5 of N/OFQ came closer to the terminal amide group of Gln286. The distance plot in Figure 8B, shows that after 2 ns of simulation, the two groups were hydrogen-bonded to each other and maintained the interaction throughout the simulation. Site-directed mutagenesis of Gln286 to Ala resulted in loss of the activation of NOP receptor, without affecting the binding affinity of N/OFQ, suggesting that this interaction is important for receptor movements during activation.[45]

Photoaffinity labeling with [Bpa^{10},Tyr^{14}]nociceptin suggested that the C-terminal residues of the N/OFQ peptide bind near the EL3 loop.[47] The MD simulation of the N/OFQ peptide with the NOP receptor in membrane bilayer suggested the movement of N/OFQ peptide from its starting position towards EL3 loop. The negatively charged residue Glu295 in the

EL3 loop showed very strong ionic interaction with R12 of N/OFQ throughout the simulation, while R8 was also observed to be involved in ionic interactions with Glu295 occasionally. This negatively charged amino acid residue is unique to the NOP receptor (analogous amino acid in MOP and KOP is Thr) and seems to be necessary for holding the positively charged core of N/OFQ peptide. This interaction brings the N/OFQ peptide in close proximity to the EL3 loop, thus verifying the experimental observation by Moulédous et al during the binding of the photoaffinity peptide. The other positively charged amino acids (K9 and K13) of N/OFQ peptide made ionic interactions with negatively charged amino acids of EL2 loop (Asp195-Glu196-Glu197) as shown in Figure 7B. The flexible K13 residue was oriented randomly, swinging from the EL2 loop (in close proximity to Asp195) and the solvent occasionally. MD simulation also suggested a movement of the N/OFQ helical portion, and strong interaction between Asp195 and K9 of N/OFQ after 2 ns of the simulation of the N/OFQ:NOP receptor complex. Table 1 lists the polar interactions made by N/OFQ with the NOP receptor.

Binding of Ro 64-6198

The compound Ro 64-6198 represents one of the more active and selective agonists amongst the 1,3,8-triazaspiro[4.5]decan-4-one series of compounds synthesized as NOP receptor ligands. Ro 64-6198 was previously docked into an inactive NOP receptor conformation based on rhodopsin, using a manual docking procedure.[3] Since Ro 64-6198 is a NOP agonist, we docked it with the active-state NOP receptor conformation in this study, to examine the interactions of this potent full agonist with the NOP receptor (Figure 9). The aromatic portion of the triazaspirodecanone of Ro 64-6198 occupied a nonpolar pocket at the extracellular end of the binding cavity comprising of hydrophobic residues Cys200, Val202, Trp116, Cys123$^{3.25}$, Val126$^{3.28}$, Ile127$^{3.29}$ and Leu104$^{2.57}$. As depicted in the figure, this pocket is relatively constrained and cannot accommodate substitutions around this phenyl ring. This is consistent with the SAR studies on the substitution pattern of this aromatic ring reported by Wichmann et al,[48] where only an unsubstituted aromatic ring had the highest affinity for the NOP receptor.

The tricyclic phenalenyl ring moiety on the piperidine is surrounded by the hydrophobic amino acids such as Tyr131$^{3.33}$, Met134$^{3.36}$, Phe135$^{3.37}$, Ile219$^{5.42}$, Phe224$^{5.47}$, Trp276$^{6.48}$, and Val279$^{6.51}$. From an analysis of the analogous pockets in the mu and kappa opioid receptors (not shown), it appears that some residues in the NOP receptor binding pocket are responsible for conferring the binding selectivity of the phenalenyl group versus other opioid receptors. Amongst these, Val279$^{6.51}$ in NOP binding pocket is distinct compared to the corresponding residue (Ile219$^{5.42}$) in the other opioid receptors. Visual analysis of the binding pose of Ro 64-6198 in NOP suggests that an Ile residue (as found in other opioid receptors, instead of Val279$^{6.51}$ found in NOP) would result in a steric clash, likely to diminish binding of Ro 64-6198 to the other opioid receptors. This is depicted in Figure 9, with an in silico mutation of Val279$^{6.51}$ in NOP to Ile. The phenalenyl ring in Ro 64-6198, therefore, appears to play a significant role in the observed selectivity of this ligand for the NOP receptor.

In previous docking studies of Ro 64-6198, a single hydrophilic interaction was shown in the heterocyclic portion of the molecule, between amide nitrogen of the triazaspirodecanone and hydroxyl group of Thr305$^{7.39}$. Our automated docking analysis of Ro 64-6198 to the active-state conformation of the NOP receptor, on the other hand, showed three possible H-bonding interactions between Ro 64-6198 and the active-state NOP receptor. The carbonyl group of triazaspirodecanone makes strong H-bonding interaction with Thr305$^{7.39}$, while the amide nitrogen makes a polar interaction with Tyr309$^{7.43}$. The polar interactions made by Ro 64-6198 with the NOP receptor are listed in Table 1. As discussed above, Tyr309$^{7.43}$ is involved in a polar hydrogen bonding network with Tyr58$^{1.39}$, Glu199 and Arg302$^{7.36}$

which stabilize the inactive conformation of the receptor. These observations strongly suggest that agonist binding likely involves breaking of several of these polar interactions that stabilize the inactive-state receptor, leading to receptor activation.

CONCLUSIONS

The first homology model of the active-state conformation of the NOP receptor has been determined from the crystal structure of the G-protein bound opsin receptor as template. In addition, a model of the inactive-state conformation of the NOP receptor is also reported. The active-state conformation showed global movements of the TM helices, compared to the inactive-state model, which appear to be consistent with an activated GPCR structure. The global toggle switch Trp6.48 and the hydrogen bonding polar network within the GPCR helical bundle that are known to be important for activation, were further refined after MD simulation of the active-state model. The involvement of Asn133 with the polar network suggests the significance of this residue in the activation process. The MD simulation of the complex of N/OFQ with the active-state NOP receptor further supports the experimental observation that N/OFQ residues 14–17 have no role in binding or activation of the receptor.

The active-state model was further validated by docking of N/OFQ, the endogenous heptadecapeptide ligand for NOP, and by Surflex-based docking of the NOP agonist Ro 64-6198. Both agonist ligands clearly showed the involvement of the EL2 loop residues in their binding. Involvement of several other active-site residues, in the binding of these two different ligands are further consistent with site-directed mutagenesis experiments reported in the literature. Our findings on the role of the EL2 loop in ligand selectivity and activation of NOP are consistent with receptor chimera data and show that unlike with other opioid receptors, NOP receptor activation involves the EL2 loop. Our studies give new insights into the activation of NOP by agonists and the selectivity of NOP ligands over the other opioid receptors. Our modeling and docking studies are valuable for the design of selective NOP ligands.

Supplementary Material

Refer to Web version on PubMed Central for supplementary material.

Acknowledgments

This work was supported by grants from the National Institutes of Health, NIDA R01DA14026 and R01DA14026-07S1.

References

1. Zaveri N, Polgar WE, Olsen CM, Kelson AB, Grundt P, Lewis JW, Toll L. Characterization of opiates, neuroleptics, and synthetic analogs at ORL1 and opioid receptors. Eur J Pharmacol. 2001; 428:29–36. [PubMed: 11779034]
2. Topham CM, Mouledous L, Poda G, Maigret B, Meunier JC. Molecular modelling of the ORL1 receptor and its complex with nociceptin. Protein Eng. 1998; 11:1163–1179. [PubMed: 9930666]
3. Broer BM, Gurrath M, Holtje HD. Molecular modelling studies on the ORL1-receptor and ORL1-agonists. J Comput Aided Mol Des. 2003; 17:739–754. [PubMed: 15072434]
4. Liu M, He L, Hu X, Liu P, Luo HB. 3D-QSAR, homology modeling, and molecular docking studies on spiropiperidines analogues as agonists of nociceptin/orphanin FQ receptor. Bioorg Med Chem Lett. 20:7004–7010. [PubMed: 20961754]
5. Lapalu S, Moisand C, Butour JL, Mollereau C, Meunier JC. Different domains of the ORL1 and kappa-opioid receptors are involved in recognition of nociceptin and dynorphin A. FEBS Lett. 1998; 427:296–300. [PubMed: 9607332]

6. Mollereau C, Mouledous L, Lapalu S, Cambois G, Moisand C, Butour JL, Meunier JC. Distinct mechanisms for activation of the opioid receptor-like 1 and kappa-opioid receptors by nociceptin and dynorphin A. Mol Pharmacol. 1999; 55:324–331. [PubMed: 9927625]
7. Ahuja S, Hornak V, Yan ECY, Syrett N, Goncalves JA, Hirshfeld A, Ziliox M, Sakmar TP, Sheves M, Reeves PJ, Smith SO, Eilers M. Helix movement is coupled to displacement of the second extracellular loop in rhodopsin activation. Nat Struct Mol Biol. 2009; 16:168–175. [PubMed: 19182802]
8. Wess J, Han SJ, Kim SK, Jacobson KA, Li JH. Conformational changes involved in G-protein-coupled-receptor activation. Trends Pharmacol Sci. 2008; 29:616–625. [PubMed: 18838178]
9. Ahuja S, Smith SO. Multiple switches in G protein-coupled receptor activation. Trends Pharmacol Sci. 2009; 30:494–502. [PubMed: 19732972]
10. Nygaard R, Frimurer TM, Holst B, Rosenkilde MM, Schwartz TW. Ligand binding and micro-switches in 7TM receptor structures. Trends Pharmacol Sci. 2009; 30:249–259. [PubMed: 19375807]
11. Blundell TL, Sibanda BL, Sternberg MJ, Thornton JM. Knowledge-based prediction of protein structures and the design of novel molecules. Nature. 1987; 326:347–352. [PubMed: 3550471]
12. Williams MG, Shirai H, Shi J, Nagendra HG, Mueller J, Mizuguchi K, Miguel RN, Lovell SC, Innis CA, Deane CM, Chen L, Campillo N, Burke DF, Blundell TL, de Bakker PIW. Sequence-structure homology recognition by iterative alignment refinement and comparative modeling. Proteins: Structure, Function, and Bioinformatics. 2001; 45:92–97.
13. Dolan MA, Keil M, Baker DS. Comparison of composer and ORCHESTRAR. Proteins: Structure, Function, and Bioinformatics. 2008; 72:1243–1258.
14. Cherezov V, Rosenbaum DM, Hanson MA, Rasmussen SG, Thian FS, Kobilka TS, Choi HJ, Kuhn P, Weis WI, Kobilka BK, Stevens RC. High-resolution crystal structure of an engineered human beta2-adrenergic G protein-coupled receptor. Science. 2007; 318:1258–1265. [PubMed: 17962520]
15. Palczewski K, Kumasaka T, Hori T, Behnke CA, Motoshima H, Fox BA, Le Trong I, Teller DC, Okada T, Stenkamp RE, Yamamoto M, Miyano M. Crystal structure of rhodopsin: A G protein-coupled receptor. Science. 2000; 289:739–745. [PubMed: 10926528]
16. Worth CL, Kleinau G, Krause G. Comparative Sequence and Structural Analyses of G-Protein-Coupled Receptor Crystal Structures and Implications for Molecular Models. PLoS ONE. 2009; 4:e7011. [PubMed: 19756152]
17. Park JH, Scheerer P, Hofmann KP, Choe HW, Ernst OP. Crystal structure of the ligand- free G-protein-coupled receptor opsin. Nature. 2008; 454:183–187. [PubMed: 18563085]
18. Qian N, Sejnowski TJ. Predicting the secondary structure of globular proteins using neural network models. Journal of Molecular Biology. 1988; 202:865–884. [PubMed: 3172241]
19. Gibrat JF, Garnier J, Robson B. Further developments of protein secondary structure prediction using information theory: New parameters and consideration of residue pairs. Journal of Molecular Biology. 1987; 198:425–443. [PubMed: 3430614]
20. Maxfield FR, Scheraga HA. Status of empirical methods for the prediction of protein backbone topography. Biochemistry. 1976; 15:5138–5153. [PubMed: 990270]
21. Phillips JC, Braun R, Wang W, Gumbart J, Tajkhorshid E, Villa E, Chipot C, Skeel RD, Kale L, Schulten K. Scalable molecular dynamics with NAMD. J Comput Chem. 2005; 26:1781–1802. [PubMed: 16222654]
22. MacKerell AD, Bashford D, Bellott, Dunbrack RL, Evanseck JD, Field MJ, Fischer S, Gao J, Guo H, Ha S, Joseph-McCarthy D, Kuchnir L, Kuczera K, Lau FTK, Mattos C, Michnick S, Ngo T, Nguyen DT, Prodhom B, Reiher WE, Roux B, Schlenkrich M, Smith JC, Stote R, Straub J, Watanabe M, Wiórkiewicz-Kuczera J, Yin D, Karplus M. All-Atom Empirical Potential for Molecular Modeling and Dynamics Studies of Proteins. The Journal of Physical Chemistry B. 1998; 102:3586–3616.
23. Humphrey W, Dalke A, Schulten K. VMD-Visual Molecular Dynamics. J Mol Graphics. 1996; 14:33–38.

24. Orsini MJ, Nesmelova I, Young HC, Hargittai B, Beavers MP, Liu J, Connolly PJ, Middleton SA, Mayo KH. The nociceptin pharmacophore site for opioid receptor binding derived from the NMR structure and bioactivity relationships. J Biol Chem. 2005; 280:8134–8142. [PubMed: 15596448]
25. Rasmussen SG, Choi HJ, Rosenbaum DM, Kobilka TS, Thian FS, Edwards PC, Burghammer M, Ratnala VR, Sanishvili R, Fischetti RF, Schertler GF, Weis WI, Kobilka BK. Crystal structure of the human beta2 adrenergic G-protein-coupled receptor. Nature. 2007; 450:383–387. [PubMed: 17952055]
26. Warne T, Serrano-Vega MJ, Baker JG, Moukhametzianov R, Edwards PC, Henderson R, Leslie AG, Tate CG, Schertler GF. Structure of a beta1-adrenergic G-protein-coupled receptor. Nature. 2008; 454:486–491. [PubMed: 18594507]
27. Jaakola VP, Griffith MT, Hanson MA, Cherezov V, Chien EY, Lane JR, Ijzerman AP, Stevens RC. The 2. 6 angstrom crystal structure of a human A2A adenosine receptor bound to an antagonist. Science. 2008; 322:1211–1217. [PubMed: 18832607]
28. Wu B, Chien EYT, Mol CD, Fenalti G, Liu W, Katritch V, Abagyan R, Brooun A, Wells P, Bi FC, Hamel DJ, Kuhn P, Handel TM, Cherezov V, Stevens RC. Structures of the CXCR4 Chemokine GPCR with Small-Molecule and Cyclic Peptide Antagonists. Science. 2010; 330:1066–1071. [PubMed: 20929726]
29. Kam KW, New DC, Wong YH. Constitutive activation of the opioid receptor-like (ORL1) receptor by mutation of Asn133 to tryptophan in the third transmembrane region. J Neurochem. 2002; 83:1461–1470. [PubMed: 12472900]
30. Lebon G, Warne T, Edwards PC, Bennett K, Langmead CJ, Leslie AGW, Tate CG. Agonist-bound adenosine A2A receptor structures reveal common features of GPCR activation. Nature. 2011; 474:521–525. [PubMed: 21593763]
31. Xu F, Wu H, Katritch V, Han GW, Jacobson KA, Gao ZG, Cherezov V, Stevens RC. Structure of an agonist-bound human A2A adenosine receptor. Science. 2011; 332:322–327. [PubMed: 21393508]
32. Pellissier LP, Sallander J, Campillo M, Gaven F, Queffeulou E, Pillot M, Dumuis A, Claeysen S, Bockaert J, Pardo L. Conformational toggle switches implicated in basal constitutive and agonist-induced activated states of 5-hydroxytryptamine-4 receptors. Mol Pharmacol. 2009; 75:982–990. [PubMed: 19168624]
33. McAllister SD, Hurst DP, Barnett-Norris J, Lynch D, Reggio PH, Abood ME. Structural mimicry in class A G protein-coupled receptor rotamer toggle switches: the importance of the F3.36(201)/W6. 48(357) interaction in cannabinoid CB1 receptor activation. J Biol Chem. 2004; 279:48024–48037. [PubMed: 15326174]
34. Kolinski M, Filipek S. Molecular dynamics of mu opioid receptor complexes with agonists and antagonists. The Open Structural Biology Journal. 2008; 2:8–20.
35. Kolinski M, Filipek S. Studies of the activation steps concurrent to ligand binding in delta and kappa opioid receptors based on molecular dynamics simulations. The Open Structural Biology Journal. 2009; 3:51–63.
36. Holst B, Nygaard R, Valentin-Hansen L, Bach A, Engelstoft MS, Petersen PS, Frimurer TM, Schwartz TW. A conserved aromatic lock for the tryptophan rotameric switch in TM-VI of seven-transmembrane receptors. J Biol Chem. 2010; 285:3973–3985. [PubMed: 19920139]
37. Scarselli M, Li B, Kim SK, Wess J. Multiple residues in the second extracellular loop are critical for M3 muscarinic acetylcholine receptor activation. J Biol Chem. 2007; 282:7385–7396. [PubMed: 17213190]
38. Conner M, Hawtin SR, Simms J, Wootten D, Lawson Z, Conner AC, Parslow RA, Wheatley M. Systematic analysis of the entire second extracellular loop of the V(1a) vasopressin receptor: key residues, conserved throughout a G-protein-coupled receptor family, identified. J Biol Chem. 2007; 282:17405–17412. [PubMed: 17403667]
39. Ott TR, Troskie BE, Roeske RW, Illing N, Flanagan CA, Millar RP. Two mutations in extracellular loop 2 of the human GnRH receptor convert an antagonist to an agonist. Mol Endocrinol. 2002; 16:1079–1088. [PubMed: 11981042]

40. Baneres JL, Mesnier D, Martin A, Joubert L, Dumuis A, Bockaert J. Molecular characterization of a purified 5-HT4 receptor: a structural basis for drug efficacy. J Biol Chem. 2005; 280:20253–20260. [PubMed: 15774473]

41. Mansour A, Taylor LP, Fine JL, Thompson RC, Hoversten MT, Mosberg HI, Watson SJ, Akil H. Key residues defining the mu-opioid receptor binding pocket: a site-directed mutagenesis study. J Neurochem. 1997; 68:344–353. [PubMed: 8978745]

42. Akuzawa N, Takeda S, Ishiguro M. Structural modelling and mutation analysis of a nociceptin receptor and its ligand complexes. J Biochem. 2007; 141:907–916. [PubMed: 17456499]

43. Dooley CT, Houghten RA. Orphanin FQ: receptor binding and analog structure activity relationships in rat brain. Life Sci. 1996; 59:PL23–29. [PubMed: 8684262]

44. Guerrini R, Calo G, Rizzi A, Bianchi C, Lazarus LH, Salvadori S, Temussi PA, Regoli D. Address and message sequences for the nociceptin receptor: a structure-activity study of nociceptin-(1–13)-peptide amide. J Med Chem. 1997; 40:1789–1793. [PubMed: 9191955]

45. Mouledous L, Topham CM, Moisand C, Mollereau C, Meunier JC. Functional inactivation of the nociceptin receptor by alanine substitution of glutamine 286 at the C terminus of transmembrane segment VI: evidence from a site-directed mutagenesis study of the ORL1 receptor transmembrane-binding domain. Mol Pharmacol. 2000; 57:495–502. [PubMed: 10692489]

46. Mollereau C, Moisand C, Butour JL, Parmentier M, Meunier JC. Replacement of Gln280 by His in TM6 of the human ORL1 receptor increases affinity but reduces intrinsic activity of opioids. FEBS Lett. 1996; 395:17–21. [PubMed: 8849681]

47. Mouledous L, Topham CM, Mazarguil H, Meunier JC. Direct identification of a peptide binding region in the opioid receptor-like 1 receptor by photoaffinity labeling with [Bpa(10), Tyr(14)]nociceptin. J Biol Chem. 2000; 275:29268–29274. [PubMed: 10880520]

48. Wichmann J, Adam G, Rover S, Cesura AM, Dautzenberg FM, Jenck F. 8-acenaphthen-1-yl-1-phenyl-1,3,8-triaza-spiro[4. 5]decan-4-one derivatives as orphanin FQ receptor agonists. Bioorg Med Chem Lett. 1999; 9:2343–2348. [PubMed: 10476866]

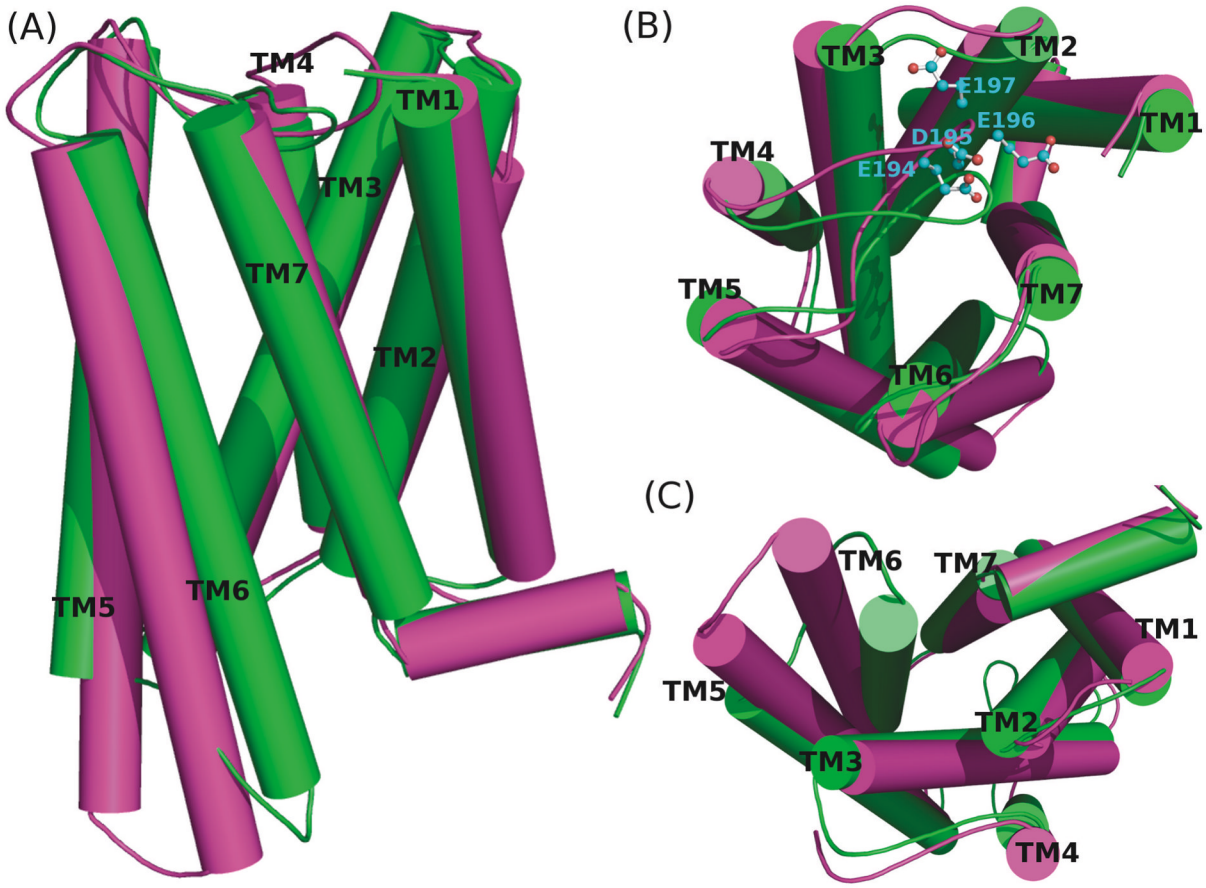

Figure 1.
Overlay of the active (magenta) and inactive (green) state of NOP receptor. (A) shows the side view, (B) extracellular view, and (C) intracellular view of the overlay.

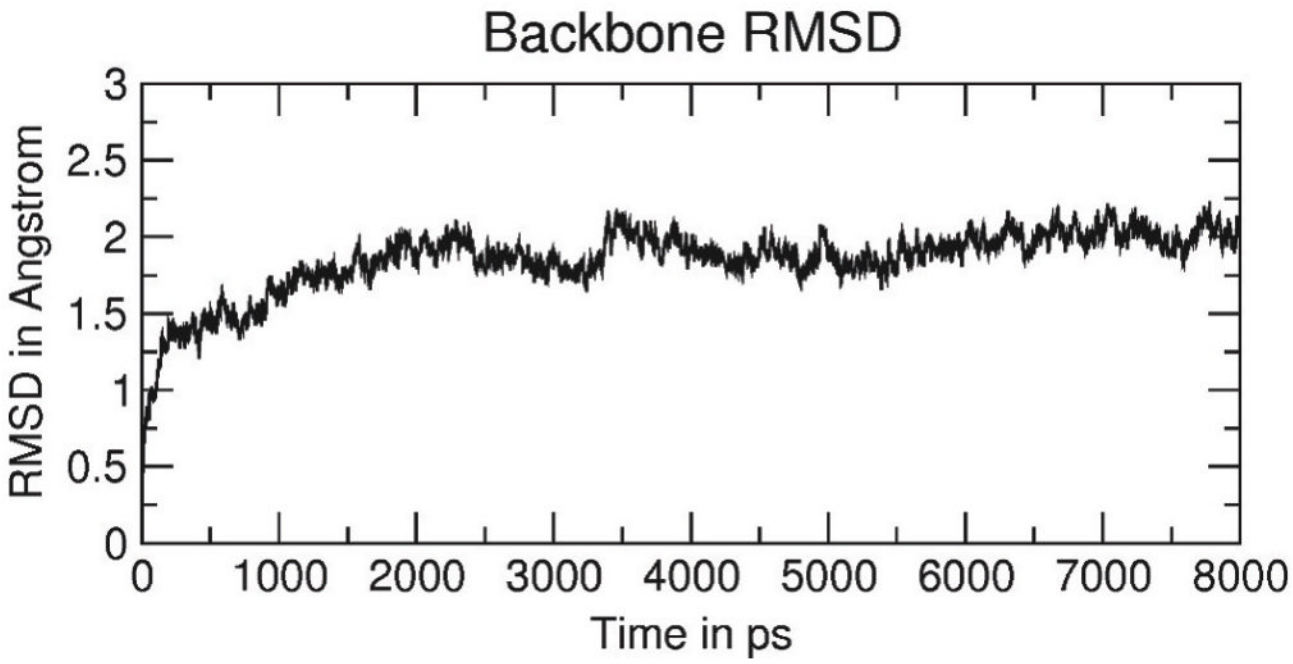

Figure 2.
Overall root mean squared deviation (RMSD) of the backbone of active-state NOP model. The RMSD of the model had stabilized after ~2.0 ns of production run. Similar RMSD profile was observed during MD simulation of inactive-state NOP model.

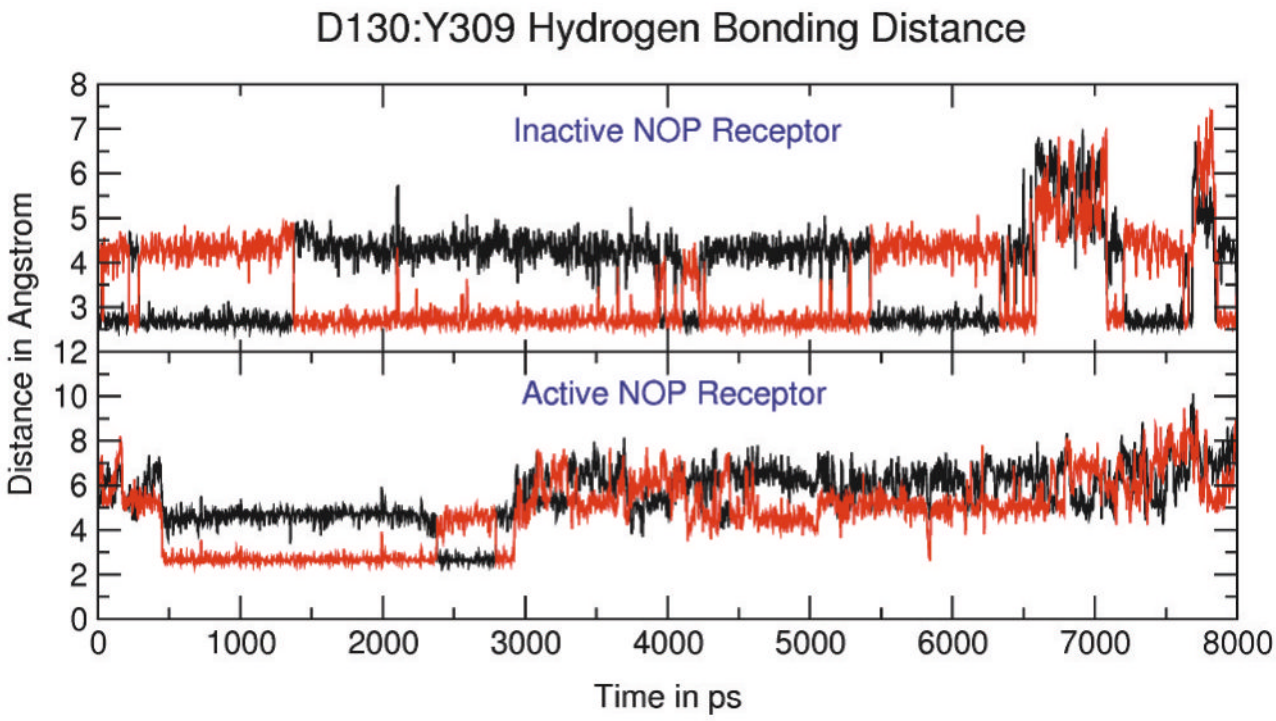

Figure 3.

Distance (in angstroms) between Asp130$^{3.32}$ side-chain carboxyl group and the terminal hydroxyl group of Tyr309$^{7.43}$ during MD simulation of the active and inactive NOP receptor models. The upper panel shows that the interaction is retained for more than 90% of the trajectory in the inactive conformation of NOP, while lower panel shows that this '3–7 lock' is disrupted after 3 ns of MD simulation of the active-state conformation. The black and red lines depict the distance between each carboxyl O of Asp130 and the OH group of Tyr309.

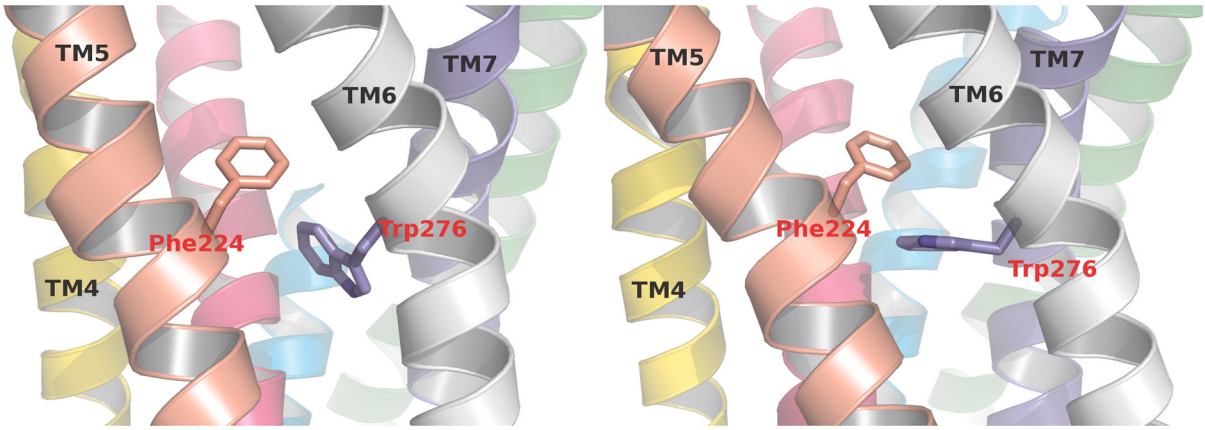

Figure 4.
The characteristic aromatic lock, showing a π-stacking of interaction of Phe224$^{5.47}$ with Trp276$^{6.48}$ in the active-state conformation of NOP receptor.

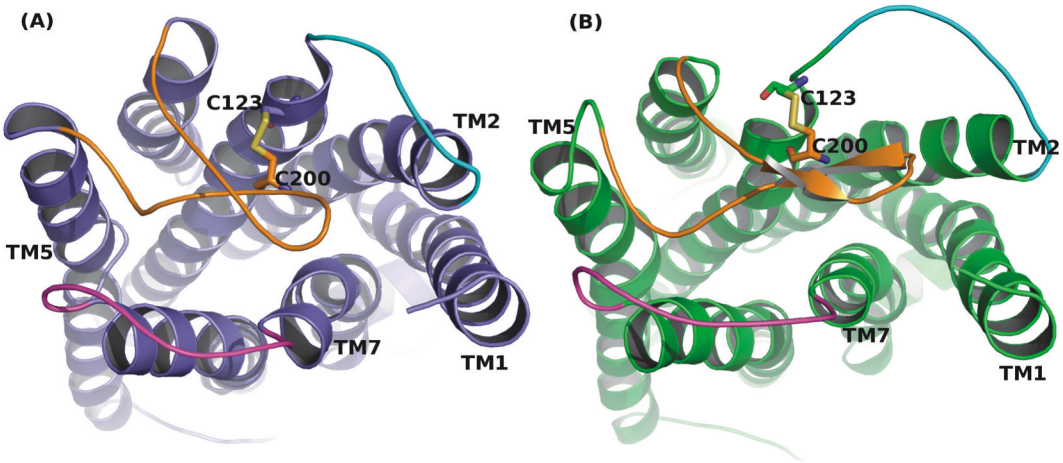

Figure 5.
Top view of NOP receptor in its inactive-state. The loops are shown in cyan (EL1), orange (EL2) and magenta (EL3) colors. (A) shows the random coil secondary structure of the EL2 loop before MD simulation. The loop acquired beta-sheet secondary structure after MD simulation, as depicted in (B).

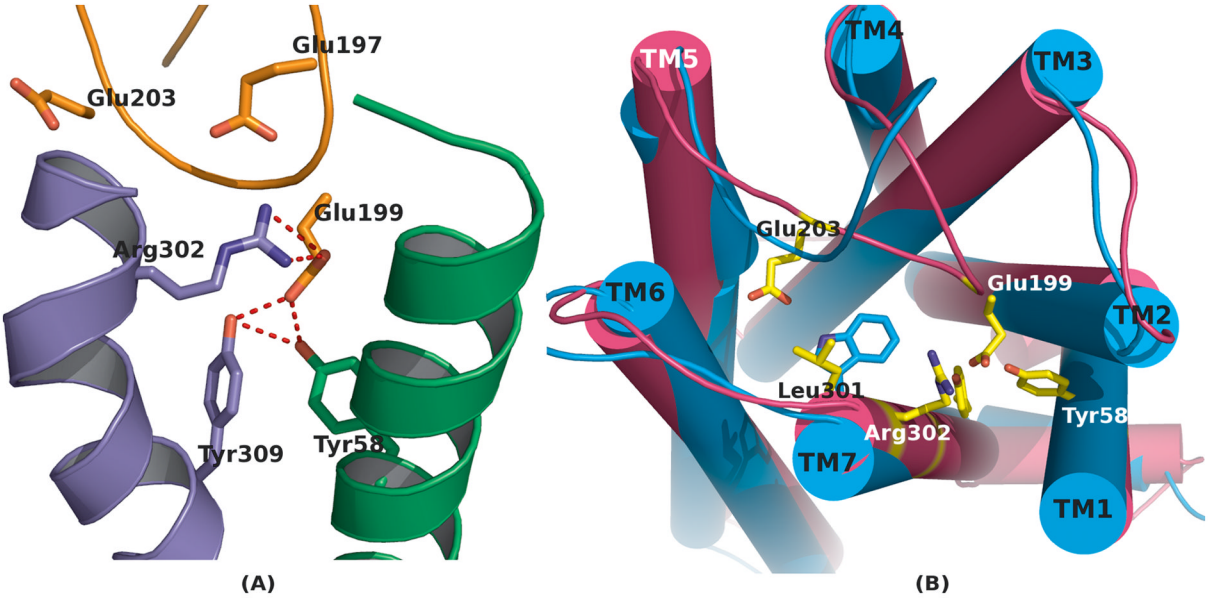

Figure 6.

(A) Observed polar hydrogen bonding network within active-state of NOP receptor model. The Glu197 and Glu199 both can be involved in the ionic interaction with Arg302$^{7.36}$. The Tyr58$^{1.39}$ and Tyr309$^{7.43}$ also make strong polar hydrogen bonding interactions with Glu199. Breaking of this polar network might be associated with ligand binding as discussed in the text. (B) Overlay of mu opioid receptor (blue) and NOP receptor (crimson red) models in their active states. The larger Trp320 residue (shown in blue stick model) of mu (and delta) opioid receptor coerces its EL2 loop to acquire a different conformation than in the NOP receptor, which contains the smaller Leu301 residue. The EL2 loop in NOP is located in close proximity of TM7, enabling a strong ionic interaction between Glu199 and Arg302$^{7.36}$. This interaction is absent in the mu opioid receptor.

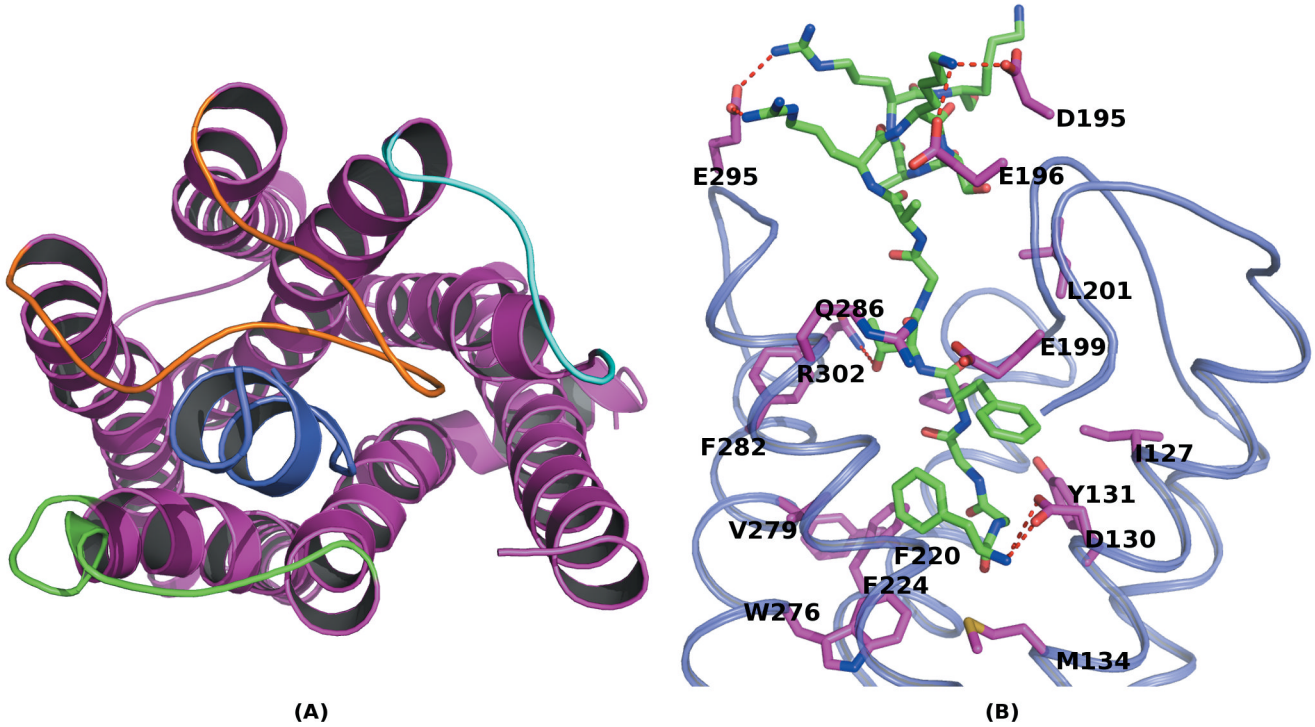

Figure 7.

(A) Top view of the N/OFQ peptide binding to the NOP receptor. Manual placement of N/OFQ peptide (shown as blue helical structure) within the active site of NOP receptor (shown in magenta). The three extracellular loops are shown in different colors (EL1: cyan, EL2: orange, and EL3: green). (B) Binding of N/OFQ(1–13) to the NOP receptor. N/OFQ is shown in green stick mode while the important NOP residues in close proximity are shown in magenta stick model. The polar interactions of N/OFQ with the receptor are shown in red dotted lines.

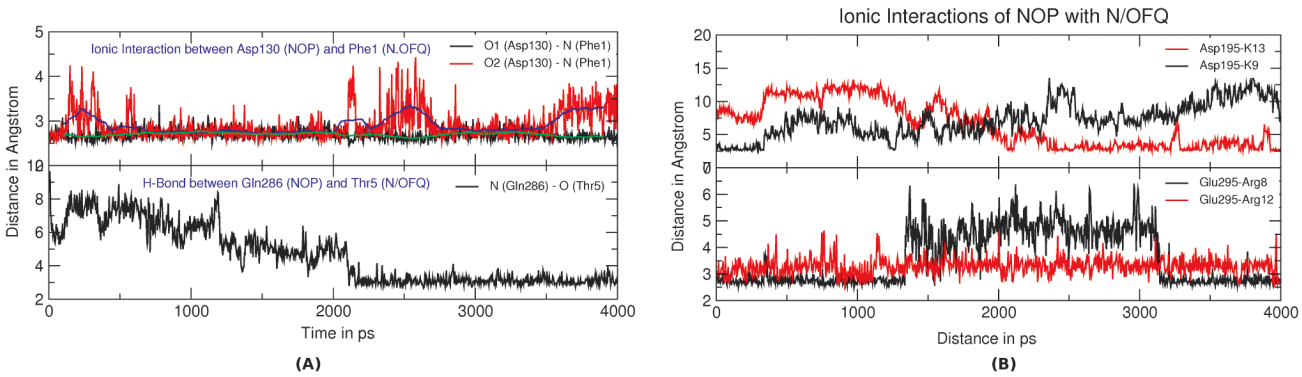

Figure 8.

(A) Non-bonding interactions within the N/OFQ and NOP receptor binding site during a 4 ns MD simulation of the complex. (Upper Panel) Strong ionic interaction between the negatively charged Asp130$^{3.32}$ and positively charged nitrogen of Phe1 of N/OFQ, maintained throughout the 4ns MD trajectory. The black and red lines depict the distance between each of carboxyl O with positively charged N in Phe1 of N/OFQ. The green and blue lines depict the same distances averaged every 50 snapshots. (Lower Panel) Hydrogen bonding interaction of between side-chain amide of Gln286 and hydroxyl group of Thr5 of N/OFQ. The two residues were ~7 Å away from each other at the beginning of the simulation; as the simulation progressed, the side-chain OH of Thr5 of N/OFQ peptide came closer to the terminal amide functional group of Gln286. (B) Ionic interactions of the positively charged core of N/OFQ with extracellular loops of NOP receptor. (Upper panel) Lys13 (N/OFQ) was in close proximity of Asp195 (EL2) in the beginning, then moved away and Lys9 (N/OFQ) approached Asp195 as the simulation progressed. (Lower panel) Ionic interaction of Glu295 (EL3) with Arg8 (N/OFQ) and Arg12 (N/OFQ). Arg8 involved in a strong ionic interaction with Glu295 throughout the MD simulation.

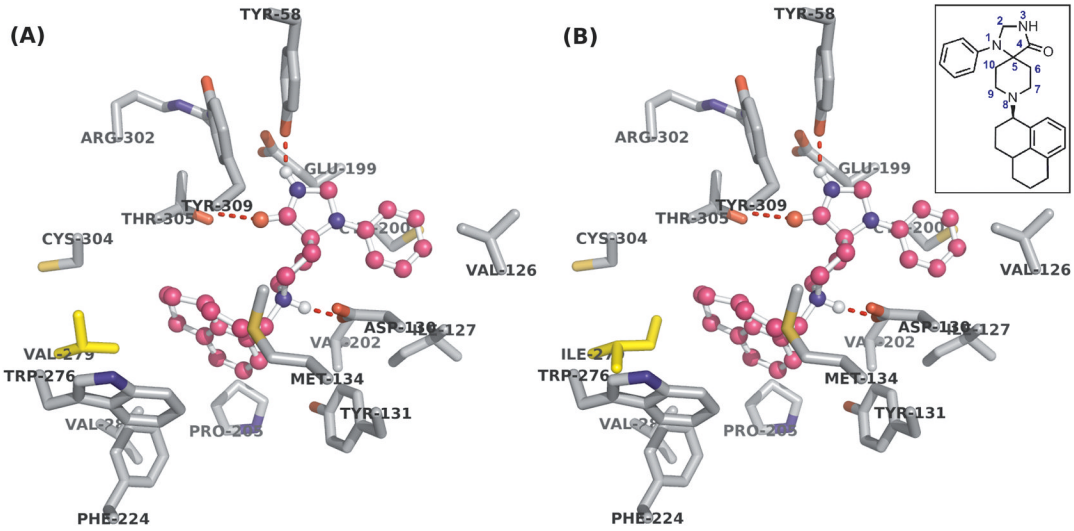

Figure 9.

(A) Binding pose of Ro 64-6198 (chemical structure inset) in the active-state NOP receptor binding site. The ligand Ro 64-6198 is shown in ball-and-stick mode (magenta colored carbon), while NOP residues are shown in grey sticks. The backbone atoms and hydrogen atoms are removed for clarity. (B) The replacement of Val279 with Ile residue (both residues shown in yellow) appears to cause a steric clash with tricyclic ring of Ro 64-6198.

Table 1

Polar interactions made by the agonist ligands N/OFQ and Ro 64-6198 with the NOP receptor active site after a 4 ns molecular dynamics simulation of the complex (also shown in Figures 7 and 9).

ID	Ligand	Interaction (Ligand…Receptor)	Distance between heavy atoms
1	Nociceptin (N/OFQ)	(Phe1)N–H…O1 (Asp130)	2.68
2		(Phe1)N–H …O2 (Asp130)	2.65
3		(Gly2)N–H …O2 (Asp130)	3.09
4		(Gly2)CO…H–O (Ser223)	3.31
5		(Thr5)H–O…H–NH (Gln286)	3.40
6		(Arg8) guanidino N–H … O1 (Glu295)	2.68
7		(Lys9) Nε–H …O1 (Asp195)	2.69
8		(Lys9) Nε–H …O1 (Glu196)	2.84
9		(Arg12) guanidino N–H …O1 (Glu295)	2.74
10	Ro 64-6198	8 N^{+}–H…O1 (Asp130)	2.81
11		8 N^{+}–H …O2 (Asp130)	3.40
12		4 C=O…H-O (Thr305)	3.30
13		3 N–H…O-C (Tyr58)	2.70